J. Fluid Mech. (1987), *vol.* 177, *pp.* 339–357
Printed in Great Britain

Bifurcation phenomena and cellular-pattern evolution in mixed-convection heat transfer

By L. FUNG, K. NANDAKUMAR AND J. H. MASLIYAH
Department of Chemical Engineering, University of Alberta, Edmonton, Alberta, T6G 2G6, Canada

(Received 7 June 1985 and in revised form 2 April 1986)

This investigation is concerned with the numerical calculation of multiple solutions for a mixed-convection flow problem in horizontal rectangular ducts. The numerical results are interpreted in terms of recent observations by Benjamin (1978*a*) on the bifurcation phenomena for a bounded incompressible fluid. The observed mutations of cellular flows are discussed in terms of dynamic interchange processes. Each cellular flow may be represented by a solution surface in the parametric space of Grashof number Gr and aspect ratio γ, which is delimited by stability boundaries. Such a stability map has been generated for each type of cellular flow by a series of numerical experiments. Once these boundaries are crossed one cellular flow mutates into another via a certain dynamical process. Although the nature of the singular points on this map have not been determined precisely, a plausible general structure of the cellular-flow exchange process emerges from this map with several features in common with the Taylor–Couette flow. The primary modes appear to exchange roles via the formation of tilted cusp. Other salient features such as primary-mode hysteresis and quasi-critical range for cellular development appear to be present. However no anomolous modes have been observed.

1. Introduction

The problem of buoyancy instability of an incompressible fluid layer was initially investigated by Bénard (1901), Rayleigh (1916), Jeffreys (1928), and Low (1929). In the theoretical work of Rayleigh, the horizontal fluid layer is assumed to be infinite in extent. The primary motion for such a simplified case is $u_i = 0$, where u_i are the velocity components. The stability of this simple primary motion could be studied analytically using linear stability theory. Subsequently, the effect of lateral bounding walls has been examined, using both linear and nonlinear theories, by Drazin (1975), Daniels (1977), Hall & Walton (1977) and Daniels (1984). Other related contributions to the Rayleigh–Bénard type of convection include Platten & Chavepeyer (1975), Behringer & Ahlers (1982) and Daniels (1981). All of these studies observed hysteresis over certain ranges of flow parameters. Cliffe & Winters (1984) have shown that Bénard convection in tilted cavities can be represented by the one-sided bifurcation for $\theta \neq 0$ (i.e. the angle of inclination from the horizontal). Pitchfork bifurcation occurs at one section of the cusp and is unstable to a symmetry-breaking perturbation. A numerical study of pure-natural-convection flows in slender vertical slots was also carried out by Lee & Korpela (1983). Dual solutions and multicellular pattern was observed.

In this work, we study the combined free- and forced-convection heat transfer in a horizontal rectangular tube with axially uniform heat flux and bottom heated–top

insulated peripheral thermal boundary conditions. This problem is of interest to mechanical and chemical engineers because of the presence of both the free and forced convection mechanisms in heat exchangers. The condition of axially uniform flux can be realized with an electrically heated duct. For the peripheral boundary condition a number of variations have been studied both experimentally and theoretically. Among the theoretical works, Morton (1959), Faris & Viskanta (1969) and Iqbal & Stachiewicz (1966, 1967) have all used a perturbation approach to study the effect of free convection on forced-convection heat transfer. Cheng & Hwang (1969), Hwang & Cheng (1970), Patanker, Ramadhyani and Sparrow (1978), Chou & Hwang (1984) and Nandakumar, Masliyah & Law (1985) have used a finite-difference method to examine the effect of a stronger free-convection mechanism. Experimental studies of the mixed-convection problem have been carried out by Hwang & Liu (1976), Hattori & Kotake (1978), Yousef & Tarasuk (1981), Osborne & Incropera (1985) and Courier & Grief (1985). These studies have revealed the existence of longitudinal rolls and heat-transfer enhancement of up to five times that associated with pure forced convection. Early work revealed a flow structure with twin counter-rotating vortices caused by buoyancy force and superimposed on the pressure-driven axial flow. First evidence of a transition to a four-cell pattern was contained in the work of Patankar *et al.*, for a circular duct with non-uniform heating. They identified a modified Grashof number as the only true dynamical parameter for this problem and observed the two-cell and four-cell pattern for the case of a non-uniform bottom-heated boundary condition. This phenomenon was later confirmed by Chou & Hwang (1984) for a rectangular geometry with uniform heating. But none of these studies revealed dual solutions and hysteresis behaviour. In a recent work by Nandakumar *et al.* (1985), a similarity among the mixed-convection flow and the pressure-driven isothermal flow in coiled ducts (the Dean problem) and the flow between rotating cylinders (the Taylor problem) was observed. It was shown that dual solutions and hysteresis behaviour are possible for both circular and rectangular geometries and for both uniform and non-uniform heating.

Recent studies on Taylor-vortex flow by Benjamin (1976, 1978*a*,*b*,*c*), Benjamin & Mullin (1981, 1982), Mullin (1982), Cliffe (1983) and Cliffe & Mullin (1985) for a finite geometry and by Meyer-Spasche & Keller (1985) for an infinite geometry with periodicity have demonstrated a very rich solution structure for that problem. Salient features of the solution structure are: (i) profuse multiplicity, (ii) anomalous modes with an odd number of cells or even cells with an odd sense of rotation, and (iii) complex bifurcation diagrams in the parameter space of aspect ratio and Taylor number. It is recognized that the mixed-convection problem under study belongs to a general class of wall-bounded instability problems which include the Taylor-vortex problem, the Bénard problem and the Dean problem. We shall show the presence of a rich structure of multiple solutions not previously demonstrated for the mixed-convection problem.

2. Governing equations

The equations of motion in the stream-function vorticity form are given below for fully developed laminar flow in a horizontal rectangular tube. The transient terms are included because a pseudotransient method is used to obtain the stationary solutions. The coordinate system and the orientation of the gravity vector are shown in figure 1.

$$\nabla^2\psi = -\Omega, \tag{1}$$

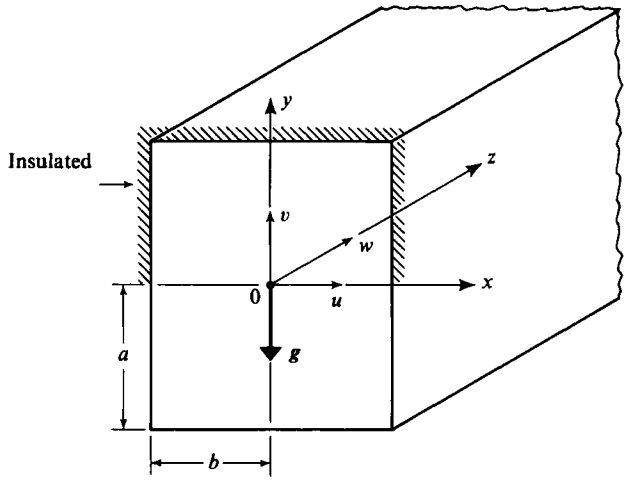

FIGURE 1. Duct geometry and coordinate system. Aspect ratio $\gamma = b/a$.

$$\frac{\partial \Omega}{\partial t} + (\boldsymbol{V}\cdot\boldsymbol{\nabla})\,\Omega = \nabla^2\Omega + Gr\frac{\partial \phi}{\partial x}, \tag{2}$$

$$\frac{\partial W}{\partial t} + (\boldsymbol{V}\cdot\boldsymbol{\nabla})w = \nabla^2 w + 1, \tag{3}$$

$$Pr\frac{\partial \phi}{\partial t} + Pr\,(\boldsymbol{V}\cdot\boldsymbol{\nabla})\phi = \nabla^2\phi - \frac{w}{\langle w\rangle}\frac{1}{4\gamma}, \tag{4}$$

where

$$(\boldsymbol{V}\cdot\boldsymbol{\nabla}) = u\frac{\partial}{\partial x} + v\frac{\partial}{\partial y}, \quad \nabla^2 = \frac{\partial^2}{\partial x^2} + \frac{\partial^2}{\partial y^2},$$

$$u = \frac{\partial \psi}{\partial y}, \quad v = -\frac{\partial \psi}{\partial x}, \quad \Omega = \frac{\partial v}{\partial x} - \frac{\partial u}{\partial y}.$$

In (4) $\langle w\rangle$ is the mean axial velocity, averaged over the flow cross-section. The viscous dissipation and compressibility effects in the energy equation are neglected. The Boussinesq approximation is invoked to account for the temperature variation of density in the body force term. The thermal boundary condition is for axially uniform heat flux with the top half of the pipe insulated and the bottom half maintained at a uniform temperature at any axial station. This peripheral boundary condition is more readily realizable than the alternative condition of the top being insulated and bottom at uniform flux. It has been attained in the recent experimental work of Osborne & Incropera (1985) on mixed-convection heat transfer between parallel plates in the entrance region. The equations have been rendered dimensionless as follows:

$$u = \frac{u'}{\nu/a}, \quad v = \frac{v'}{\nu/a}, \quad w = \frac{w'}{(-\mathrm{d}p'/\mathrm{d}z')\,(a^2/\mu)},$$

$$p = \frac{p'}{\rho(\nu/a)^2}, \quad x = \frac{x'}{a}, \quad y = \frac{y'}{a}, \quad \phi = \frac{T - T_w}{Q'/k}, \quad t = \frac{t'}{a^2/\nu}.$$

Following Patankar *et al.* (1978), the modified Grashof number, $Gr = Q'g\beta a^2/k\nu^2$ is used to characterize the natural-convection effects instead of the conventional

(Re, Ra) group as used by Cheng & Hwang (1969). These two numbers are related by, $ReRa = 8Gr$. The Q' in the above definition is the heat transfer rate per unit length of the tube given by $Q' = \rho C_p A \langle w' \rangle (\partial T/\partial z)$, A is the flow area, C_p is the specific heat of the fluid, T_w is the wall temperature, g is the gravitational constant, β is the thermal coefficient of expansion, k is the thermal conductivity, and ν is the kinematic viscosity. The boundary conditions for the stream function and vorticity arise out of imposing the no-slip condition on the wall. No symmetry boundary condition was imposed along $x = 0$ in anticipation that odd-cell modes may be possible for the problem.

The thermal boundary conditions are

$$\frac{\partial \phi}{\partial n} = 0 \quad \text{for the insulated portion of the wall,} \tag{5a}$$

$$\phi = 0 \quad \text{for the heated wall.} \tag{5b}$$

Once the flow and temperature fields satisfying the above conditions are obtained, a macroscopic force and energy balance provides the Fanning friction factor and the heat-transfer coefficient, which are of engineering importance, but can also serve as state functions useful in discriminating between multiple solutions. They are given by

$$fRe = \frac{8\gamma^2}{(1+\gamma)^2 \langle w \rangle}, \tag{6}$$

where Re is the Reynolds number and f is the Fanning friction factor. The average Nusselt number is calculated from

$$\langle Nu \rangle = \frac{2\gamma}{(1+\gamma)^2} \cdot \frac{1}{\langle \phi_b \rangle}, \tag{7}$$

where $\langle \phi_b \rangle$ is the dimensionless bulk mean temperature. The Nusselt number and Reynolds number are based on the equivalent diameter,

$$D_e = \frac{4ab}{(a+b)}. \tag{8}$$

3. Method and accuracy of solution

Equations (2)–(4) were cast into a finite-difference form by using central difference for the time derivatives, the Arakawa (1966) method for the convective terms, and the DuFort & Frankel (1953) method for the diffusive terms. The Arakawa method has a formal truncation error E of $O(\Delta t^2, \Delta x^4, \Delta y^4)$ and identically conserves Ω, Ω^2 and the kinetic energy u^2+v^2, which, as pointed out in Roache (1972), make it especially suitable for hydrodynamic instability problems. This scheme has been used by Lee & Korpela (1983), Wirtz & Liu (1975), Horne & O'Sullivan (1974), Quon (1972), and Festa (1970) in natural-convection studies.

Equation (1) is of the form of the Poisson equation and is discretized using second-order central-difference approximations. The resulting set of algebraic equations were solved using the Gauss–Seidel method with successive over-relaxation. The majority of the calculations were carried out with 21 grids in the vertical direction and up to 201 grids in the horizontal direction. Lee & Korpela (1983) used the Courant condition to obtain suitable time-steps. In this study, it was found that the appropriate Δt is 1×10^{-3} for low Gr and 7×10^{-4} for up to $Gr = 25000$. The number of time-steps required to reach steady state depends on the initial state, the γ-value,

the grid mesh, and whether a change in cellular mode is involved. For example, at $(Gr, \gamma) = (15000, 6.0)$, with a mesh of 121×21, 4000 steps were required to reach the steady four-cell flow from the initial four-cell flow at $(Gr, \gamma) = (10000, 6.0)$ when $\Delta t = 7 \times 10^{-4}$ was used. The convergence criteria for steady flow are that the Nusselt number and fRe-value do not change by more than 1×10^{-3} over 500 time-steps and that the average residuals for stream function, vorticity, axial velocity, and temperature are monotonically converging over time. Computations were done using an Array Processor FPS-164 attached to an Amdahl 5860 main frame. Double-precision arithmetic was used throughout and the computational time per time-step was 0.84 ms of central-processor time per grid point.

As for the grid-mesh requirement, at least 15 grid points per cell were provided, although rectangular grids were used for large aspect ratios. To test the adequacy of grid resolution, an 81×21 grid and a 121×21 grid were respectively used in computing the four-cell flow at $(Gr, \gamma) = (15000, 6.0)$. It was found that the fRe-values agreed to within four significant figures at 21.49, whereas $\langle Nu \rangle$ changed from 6.448 to 6.461, which was a difference of about 0.2 %. Lee & Korpela (1983) used an identical numerical scheme on a pure-natural-convection problem and tested the grid sensitivity using 9×9, 17×17 and 33×33 grids. They found 17 grid points across the narrow side of the duct to be adequate to resolve the cellular flows. Our experience with a few test cases confirms their observation.

Another aspect of our numerical study is concerned with identifying the stability boundaries of each type of cellular flow in the parameter space of aspect ratio and Grashof number. This is achieved using a bisection method in the following manner. Starting with a converged steady solution with a certain number of cells at a given (γ, Gr), one of the parameters (say Gr) is changed by small increments until the cellular pattern loss stability and converges to a steady solution with a different number of cells. Both the initial and final steady solutions (i.e. at two different parameter values) are subject to the same stringent convergence criteria outlined earlier. However, the range of parameter values over which the flow transition occurs is further refined by interval halving. While this scheme is conceptually simple to implement, it is computationally very demanding. Hence the stability boundaries have not been determined with very high precision. The bisection method was continued until the uncertainty in the Grashof number was reduced to 5 % and that in the aspect ratio was reduced to ± 0.05. More recently efficient numerical methods using a continuation method and extended systems have been used by Cliffe (1983) for the Taylor problem and by Winters & Brindley (1984) for the Dean problem. Winters & Brindley computed the critical Dean number for a semi-circular duct to be 105.6 using the continuation method. This is in excellent agreement with an earlier prediction of 105 by Masliyah (1980) using the bisection method. Hence the stability boundaries determined by the bisection method are reliable. However it appears that a deeper insight can be gained about the nature of the instability by using the extended systems.

4. Results and discussion

The numerical investigation is directed along two lines. First, the effect of aspect ratio on the flow behaviour is examined, and secondly, the range of stability of a few cellular modes is studied. Stability boundaries have been determined from numerical experiments and the results are interpretated as plausible bifurcation structures observed for similar problems.

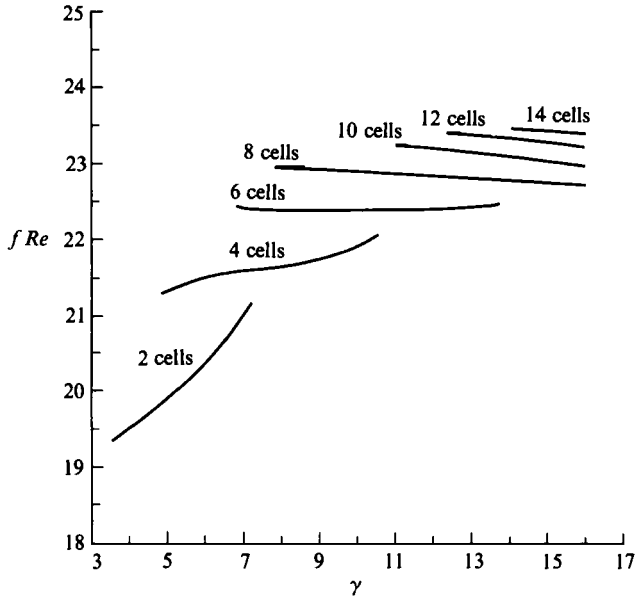

FIGURE 2. Friction-factor variation with aspect ration indicating multiple solutions at $Gr = 15000$.

4.1. *Effect of aspect ratio*

The numerical experiments were performed initially for a number of aspect ratios γ, while the Grashof number and Prandtl number were kept at 15000 and 0.73 respectively. A steady-state solution of cellular flow for each aspect ratio was then obtained by forward time marching. A number of cellular modes were thus generated, each at a particular γ. It was found that for aspect ratios of 4, 6, 8, 12 and 16, such impulsive starts cause the formation of two-cell, four-cell, six-cell, ten-cell, and twelve-cell modes respectively. At this point, the term 'impulsive start' needs to be qualified. At time zero, a hydrodynamically developed axial velocity profile was used with the cross-stream velocity components equal to zero (no natural convection). The thermal boundary conditions together with governing equations were imposed for $t \geqslant 0$. The solution is for a fully developed section far downstream from the thermal entrance region. Thus, an impulsive start refers to the imposition of a fixed Grashof number (15000 in our case) for $t \geqslant 0$ on an initial flow profile corresponding to $Gr = 0$.

Once the cellular modes were established, the stability limits were obtained by varying the aspect ratio. Owing to the computational effort required, the range of aspect ratios studied is limited to between 4 and 16. The steady-state solution at a particular aspect ratio is used as the initial condition which is again time marched to a new steady-state solution at the current γ. A critical point is reached beyond which the particular cellular mode becomes unstable. As this point is approached, small increments of γ were used so that it may be located accurately. The six-cell mode may be considered as an example. Initially a steady-state solution of six-cells is established at an aspect ratio of 8. This is then both increased and decreased to search for the upper and lower limits of stability. It was found that these limits were at $\gamma = 13.7$ and 6.9 respectively. Thus, the state curve for the six-cell mode delimited by the two limit points may be drawn for certain representative functionals of the

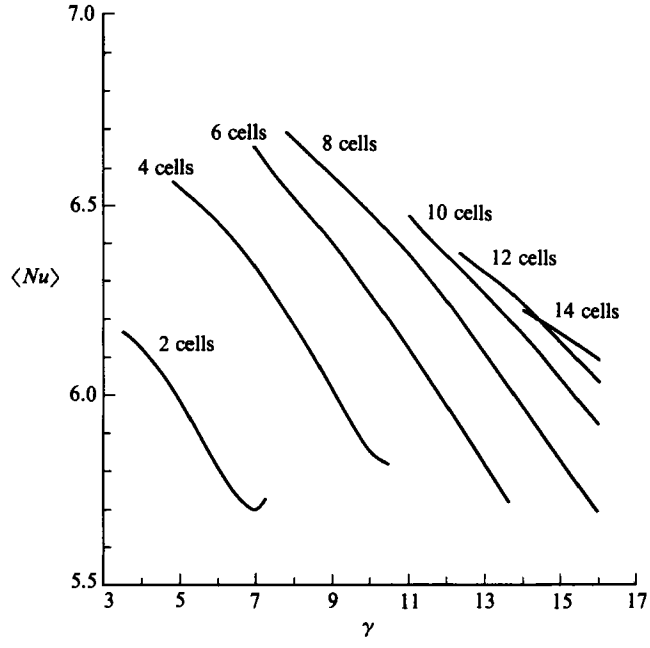

FIGURE 3. Nusselt-number variation with aspect ratio at $Gr = 15000$

problem. The friction factor fRe, and the average Nusselt number $\langle Nu \rangle$ for the various modes are shown in figures 2 and 3. For a particular cellular flow, the friction factor is not a strong function of aspect ratio. However, its value increases as the number of cells increases. The Nusselt number decreases with increasing γ for a cellular mode, but increases with the number of cells for a particular value of γ. In the region tested, there is one cross-over of Nusselt-number-state loci. It occurs at the lower range of the fourteen-cell mode. Below the cross-over, the twelve-cell mode will have higher Nusselt-number values. The upper stability limits for the eight-cell, ten-cell, twelve-cell, and fourteen-cell modes were not located since they were beyond $\gamma = 16$, which was the chosen upper bound of the current investigation.

It is seen in figures 2 and 3 that multiple steady-state solutions can exist for one set of parameters (Gr, γ, Pr). For the range of aspect ratios tested, up to four isolated solutions can exist. For the chosen fluid ($Pr = 0.73$), these represent four isolated points in the state function (Gr, γ)-parametric space which project onto a single point in the (Gr, γ)-plane. One such instance ($\gamma = 15$) is shown in figure 4 in which the stream function, axial velocity, and temperature contours are plotted. It is noted that the interior cells are approximately of the same size, with the boundary cells almost twice their length. The convection cells have the effect of creating a series of alternating hot and cold regions† in the bottom portion of the duct. These correspond respectively to the upward- and downward-flow regions. In the upward-flow regions heat is effectively convected away from the heated boundary, whereas the downward flow pushes fluid against the bottom heated boundary. As will be discussed later,

† The primary concern here is the temperature variation in the x-coordinate direction. Hence, the hot and cold regions refer to the local maximum and minimum of temperature along a horizontal plane.

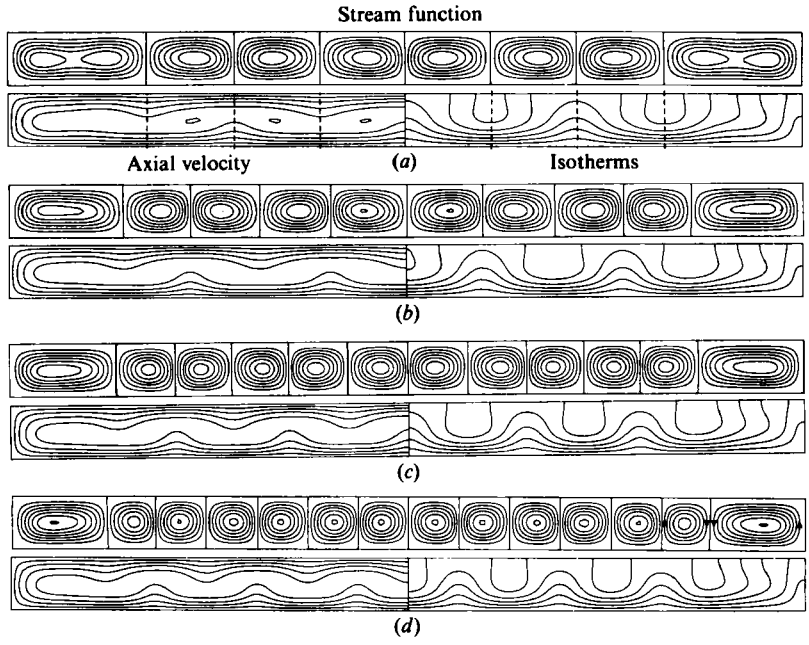

FIGURE 4. Stream function, axial velocity and isotherms for four steady solutions with (*a*) eight (*b*) ten, (*c*) twelve and (*d*) fourteen cells at $\gamma = 15$ and $Gr = 15000$.

this has some subtle consequences on a certain form of the observed bifurcation phenomena. The locus of maximum axial velocity along each vertical line becomes sinusoidal, being shifted upward or downward by the cellular circulation.

The stream function, isotherms, and axial-velocity contours for the six-cell mode for a series of aspect ratios are shown in figure 5. As the aspect ratio increases, the end cells become bi-focal, with a saddle-type stagnation point developing in the centre of the end cells. While the profiles shown in figure 5 represent stable solutions, the stability limit for six-cell solutions at a fixed Gr of 15000 is between 6.9 and 13.7. Hence any further small increase in the aspect ratio (to say 13.8) sets a dynamic process in motion where one additional cell germinates at the lower plate near the region labelled d and can grow easily into the stagnation region, thus dividing the end cell. These bi-focal end cells are responsible for the end-cell-type mutation which always results in an increase of four cells. The sharing of space between the interior cells and the end cells as γ is varied is shown in figure 6. The ratio h_e/h_m, where h_e is the average end-cell length and h_m is the average interior-cell length, is plotted against γ for a number of cellular modes. Away from the limit points, for the lower cellular modes (four-cell, six-cell, and eight-cell), the end-cell length increases at a lower rate than the interior-cell length with increasing γ, i.e. h_e/h_m decreases with γ. The rate of decline lessens with the increasing number of cells. For the ten-cell mode, this trend is only marginally observable, and for the twelve-cell and the fourteen-cell modes, it is reversed. Close to the critical points, h_e/h_m increases with γ. This corresponds to the cellular adjustment prior to the end-cell-type bifurcations.

4.2. *Cellular-flow adjustment*

Whenever multiple solutions were possible at a given set of parameter values, the mode selection would depend on the initial condition and the type of excitation

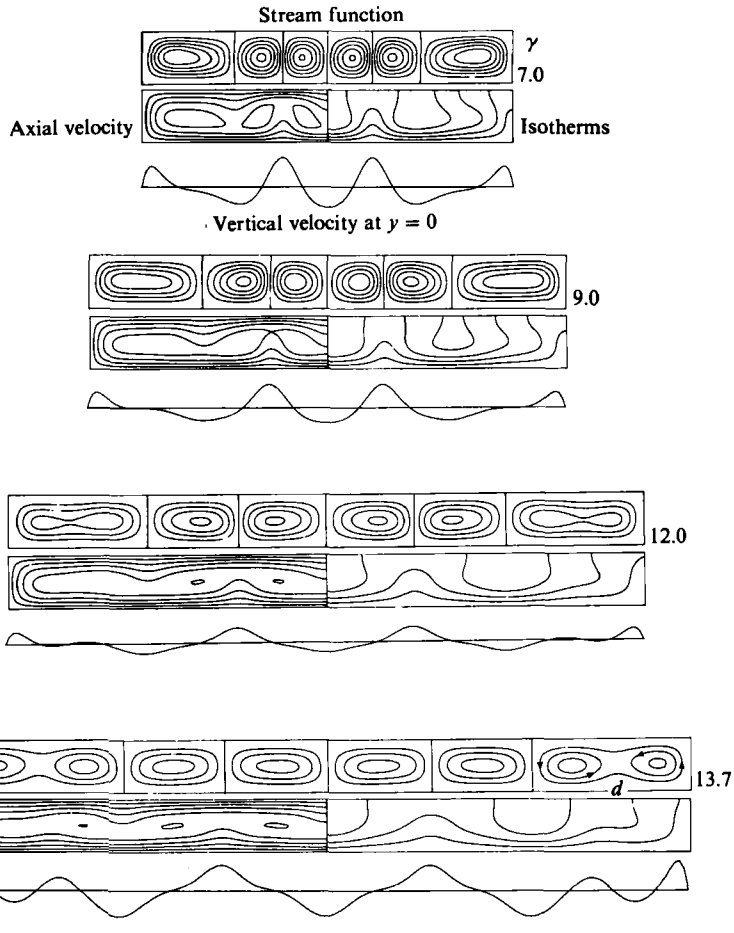

FIGURE 5. Flow field for the six-cell mode at $Gr = 15000$ as the aspect ratio is increased.

imposed on the system via a change in either one or both of the parameters. This will be demonstrated with two examples. In the first case, the converged four-cell mode at $\gamma = 9.5$ and $Gr = 10000$ is taken as the initial condition. A new solution is sought by changing γ to 10.0 at $t = 0$. In the second case, a converged four-cell mode at $\gamma = 10.0$ and $Gr = 15000$ is taken as the starting point whereby Gr is reduced to 10000 at $t = 0$. Hence, both processes have the same end state ($Gr = 10000$, $\gamma = 10.0$), both cross the upper-limit curve for the four-cell mode (see figure 10 which illustrates the stability limits for each cellular flow and it will be discussed in some detail later), but they give rise to two different cellular modes; an eight-cell mode for the former case, and a six-cell mode for the latter.

The flow and temperature profiles for the first case are shown in figure 7. The bi-focal end cells, which are stable at $\gamma = 9.5$, begin to sever at the middle where a stagnation zone has developed. The flow on either side of this zone has the same sense of rotation. The condition is stabilized by the germination of a counter-rotating vortex in between these two cells. The mutation is completed by the eventual adjustments of these new cells with the existing cells to form a new steady-state flow. Since this process involves the mutation of the end cells, it will be referred to as the 'end-cell-type' mutation. It should be noted that the slight asymmetries observed in figure 7 are an artifact

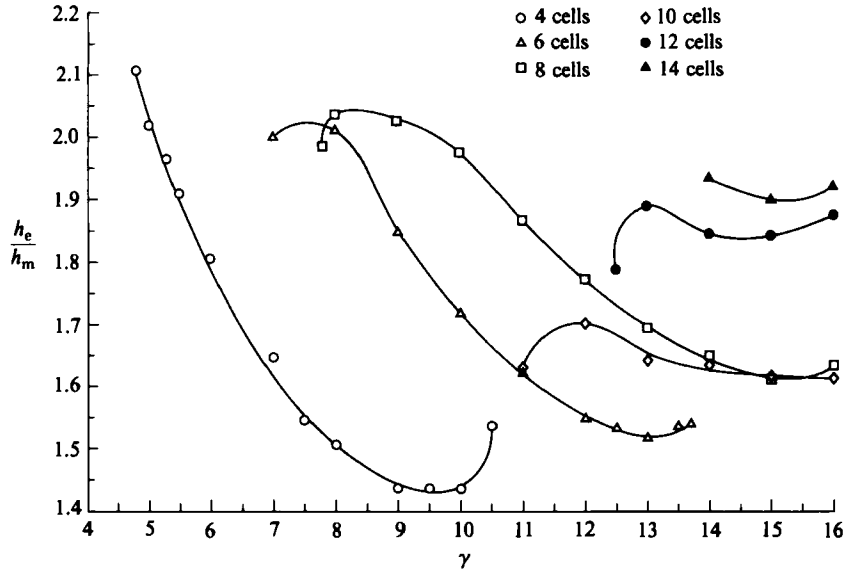

FIGURE 6. The variation of the ratio of end-cell length to interior-cell length with aspect ratio at $Gr = 15000$.

of the explicit numerical scheme. As the transient effects die down, symmetry is restored.

The second case, shown in figure 8, goes through a rather interesting mutation process. The starting steady flow is similar to the former case, but this time Gr is changed from 15000 to 10000. Initially, the end cells respond in the same manner by elongating and severing in the middle. However, another peculiar process is concurrently proceeding at the bisector of the pipe section. The reduction of Gr weakens the upward flow near the centre because of the parallel reduction in buoyancy force, which allows the accumulation of heat at that spot. This combination of events causes the formation of another vortex pair which eventually strengthens and suppresses the 'end-cell-type' mutation. As a result, the four-cell mode mutates into a six-cell mode at which a steady state is established through a final cellular adjustment phase. Since mutation in this case occurs at an interior warm region, it may be referred to as the 'interior-hot-spot-type' mutation. The vertical velocity decreases at the bisector and then collapses to a local minimum. It is noted that the downward-flow regions are not significantly affected by the reduction in Gr. The lower stability limit for the ten-call mode is $\gamma = 11.0$ at $Gr = 15000$. Therefore, it is likely that the ten-cell mode is not stable at $Gr = 10000$ and $\gamma = 10.0$. Otherwise for a large change in parameter values, it is possible for both of the processes to carry through to completion, thus forming a ten-cell mode. Such processes have been observed for a sufficiently large change in parameter values. However for small changes in parameter values across stability boundaries, the change in the number of cells occurs either through the end-cell or interior-cell mutation.

Note that when there are six cells, the warm region with upward flow does not occur at the line of symmetry (as with four-cell flow), but is located at the first cellular boundary away from the bisector. There are two of these regions, one on each side of the bisector. One such example is shown in figure 9. The initial state corresponds to a steady six-cell mode at $Gr = 15000$ and $\gamma = 13.5$ and the Gr is reduced to 10000

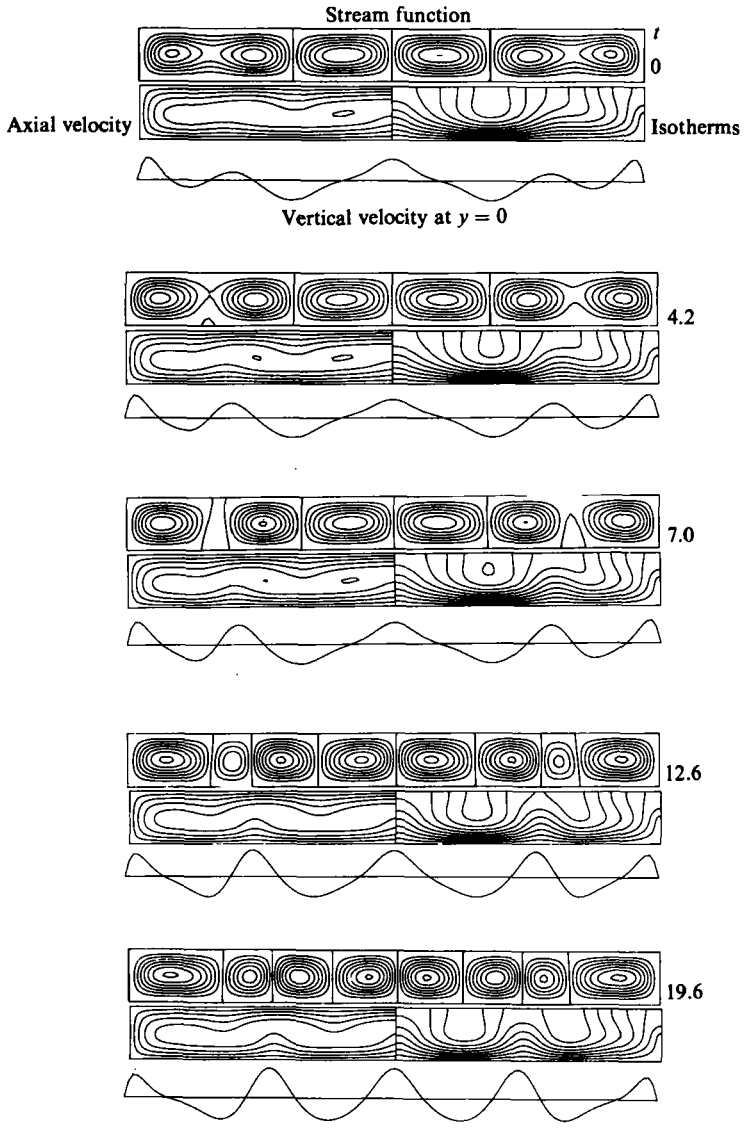

FIGURE 7. Flow field illustrating an end-cell type of bifurcation from a four-cell to an eight-cell pattern at $Gr = 10000$ when the aspect ratio is changed from 9.5 to 10.0.

at $t = 0$. A pair of cells germinate and grow in each upward-flowing warm region in the interior of the duct. Both vortex pairs thus formed remain stable and the six-cell mode evolves into a ten-cell mode.

4.3. *Quasi-critical range of Grashof number*

As pointed out earlier, the effect of lateral bounding walls on the cellular-flow evolution in the pure-natural-convection problem has been studied by Hall & Walton (1977), Daniels (1977, 1984) and Cliffe & Winters (1984). Hall & Walton (1977) have shown that, for slightly imperfect insulators as vertical boundaries, the concept of sharp bifurcation at a critical Rayleigh number is not tenable and that the onset

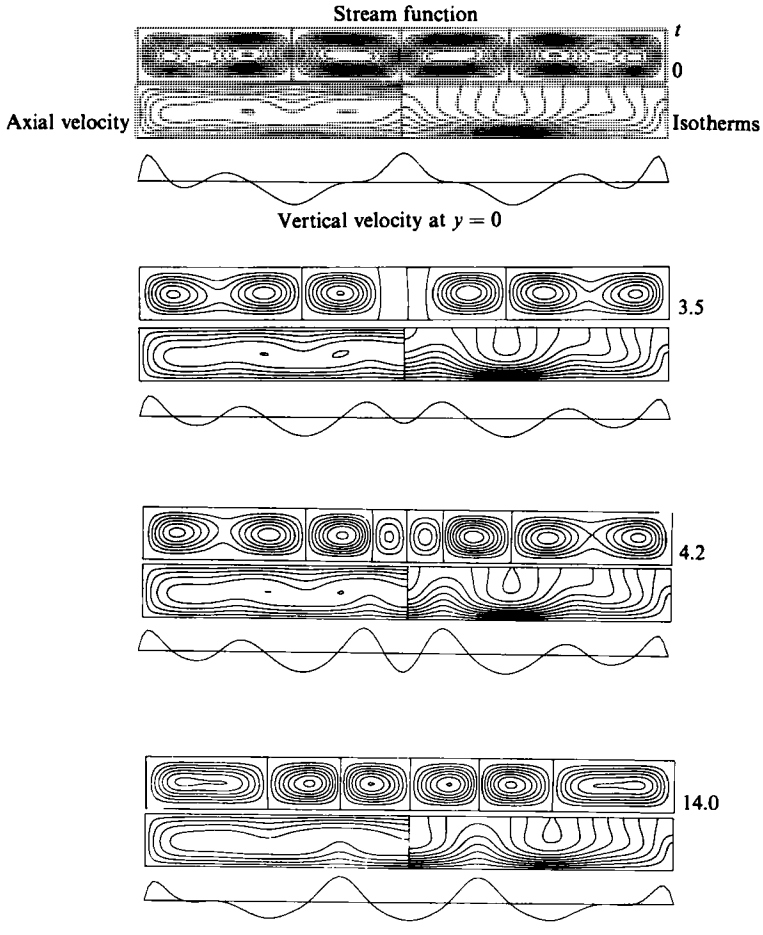

FIGURE 8. Flow field illustrating an interior-cell type of bifurcation from a four-cell to a six-cell mode at $\gamma = 10$ as Gr is changed from 15000 to 10000.

of convection is smooth. Cliffe & Winters (1984) have considered the effect of angle of inclination θ for the same problem. They have shown that, for an adiabatic endwall, a pitchfork bifurcation occurs for $\theta = 0$, but the cellular evolution is smooth for $\theta \neq 0$. In both cases, the critical behaviour is removed by the presence of a horizontal temperature gradient. In the mixed convection problem, a horizontal temperature gradient will always be present because of the forced-convection term $(w/4\gamma\langle w\rangle)$ in (4). Thus two endcells will always be present even if the vertical walls are perfect insulators – the cells, however, may be much weaker than for the present boundary conditions. The same can be expected whether the bottom wall is maintained at constant flux or constant temperature. The only exception to this is when the vertical walls are insulated and the top and bottom walls are maintained at constant (but different) temperatures. Then, in the fully developed region, there is no net axial convection and the forcing term in (4) becomes zero. The forced convection then becomes uncoupled from the natural convection and the results of the Bénard problem then became applicable. A smooth development of cells is also observed in both the Taylor and Dean problems.

In the present problem, as Gr is gradually increased, two cells are always observed.

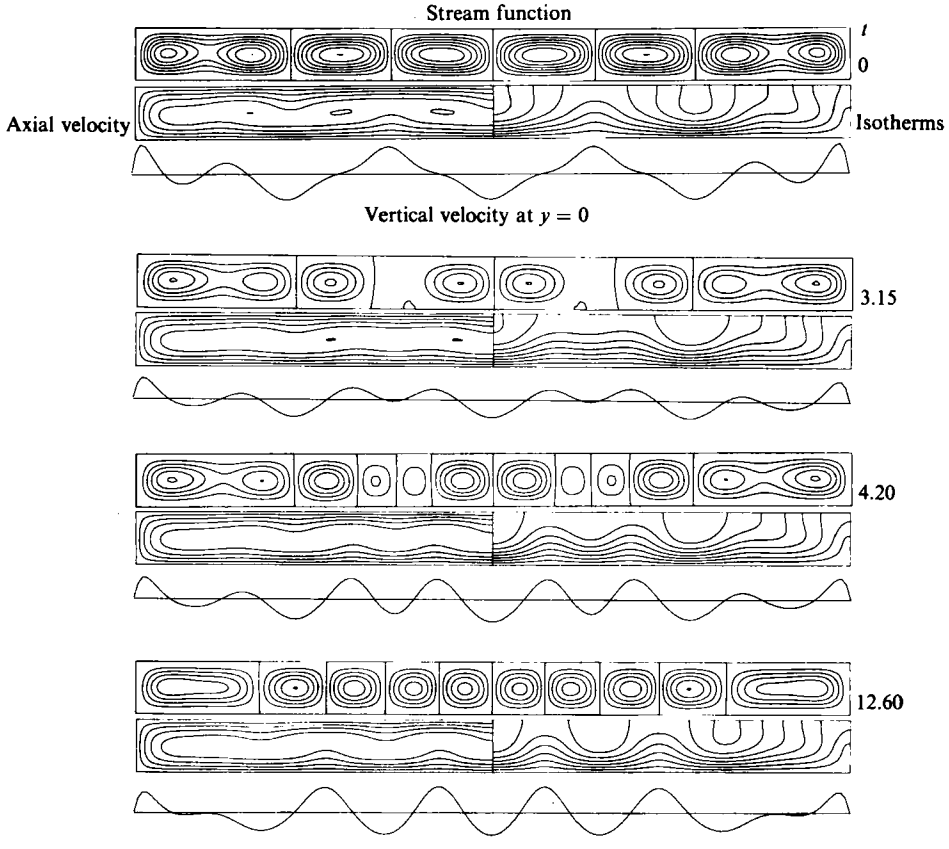

FIGURE 9. Flow field illustrating an interior-cell type bifurcation from a six-cell to a ten-cell mode at $\gamma = 13.5$ as Gr is changed from 15000 to 10000.

When the aspect ratio is large, they are confined to the ends. Interior cells begin to take shape as Gr is increased through a quasi-critical range.

In figure 10, the incipient germination of interior cells is shown as the dashed curve BE. This curve does not represent the locus of any critical or limit point; it merely indicates the zone of interior-cell development. This curve may be subdivided into segments, each corresponding to a particular primary cellular mode. For example, between γ values of 6.5–8.7, when Gr is increased through the quasi-critical range, the four-cell mode is formed. Between γ values of 8.7–11.8 the six-cell mode will be formed, and so on. It is found that for the cases tested, the primary modes always have an even number of cells and they differ from the adjacent primary modes by 2. This study did not reveal any of the anomalous modes (odd-cell modes) demonstrated by Benjamin & Mullin (1981) in their Taylor-vortex experiments. No special effort was made to realize such anomalous modes in our numerical experiments. At present, it is not known whether stable odd-cell modes can be obtained numerically for this problem, or whether they are physically realizable. However, an experimental study of natural-convection flow in enclosures of moderate aspect ratio by Linthorst, Schinkel & Hoogendoorn (1980) has demonstrated that only even-cell flows are possible.

The Nusselt number and fRe-values for a number of aspect ratios are shown in

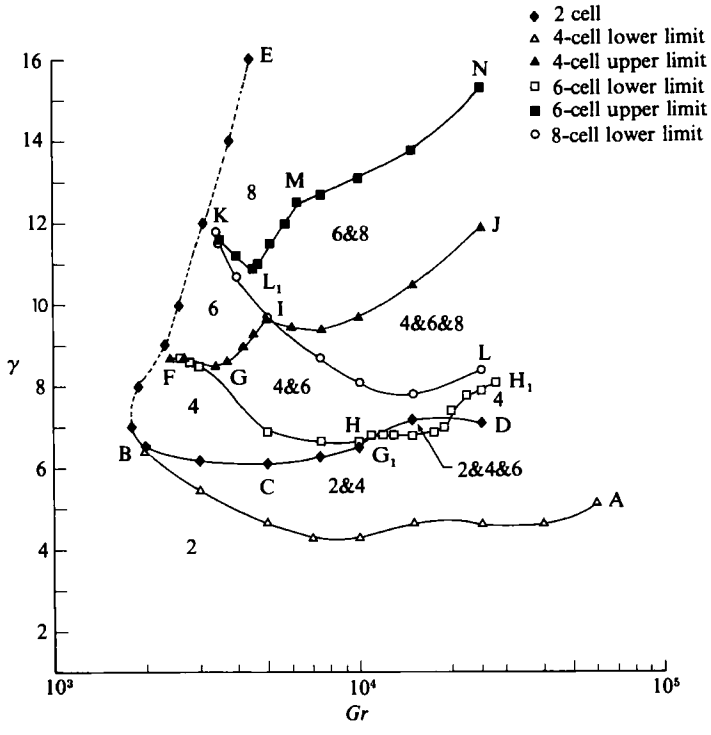

FIGURE 10. Regions of multiplicity for the two-cell, four-cell, six-cell and eight-cell modes in the range of $Gr \in (1000, 25000)$ and $\gamma \in (4.0, 16.0)$.

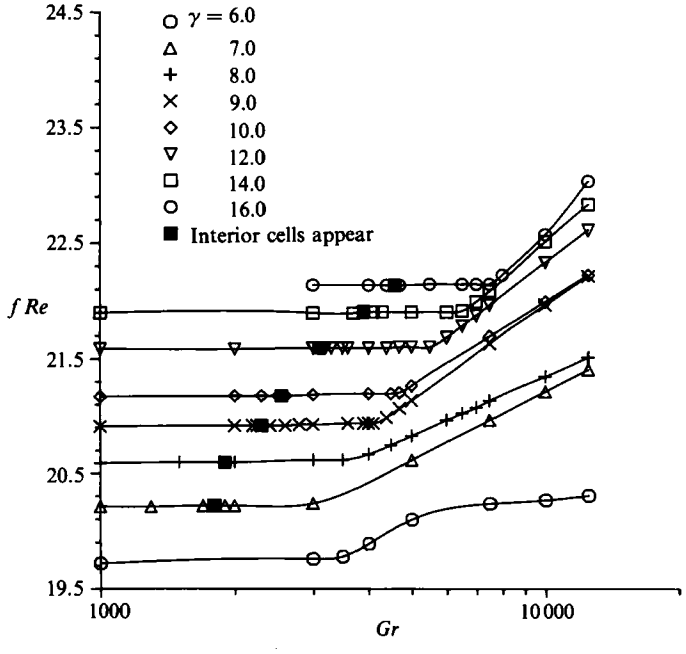

FIGURE 11. Friction-factor variation with Gr for various values of γ through the quasi-critical range.

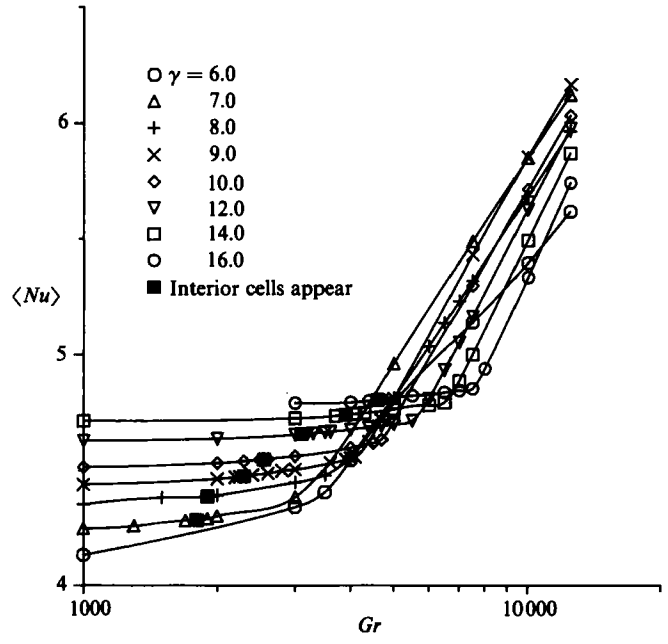

FIGURE 12. Nusselt-number variation with Gr for various values of γ through the quasi-critical range.

figures 11 and 12. The change in these functionals through the quasi-critical range is gradual. (This is especially true for the lower aspect ratios.) This further confirms that the development of a particular primary mode is not instantaneous, and that there is no exact critical value of Grashof number as such at which buoyancy instability overcomes viscous effects.

4.4. *Primary-mode exchange process and cusp catastrophe*

The stability boundaries for the two-cell, four-cell, six-cell, and eight-cell modes are shown in figure 10. For each mode, there are two limits, which will be called the upper- and lower-limit curves. The former refers to the locus where a particular cellular flow becomes unstable if the γ-value is exceeded. Similarly, the latter refers to the locus where a particular cellular form becomes unstable if the γ-value is further reduced. The upper boundary for the eight-cell mode is not located in this study.

Figure 10 can be thought of as the two-dimensional projection on the (Gr, γ)-plane of the edges of a surface representing the state of the system as a function of the control parameters Gr and γ. This stability map is incomplete in the sense that unstable solution branches as well as the type of singularity could not be determined with the present numerical method. Such solutions can be obtained by using the continuation method together with certain extended systems to determine the type of singularities (see Cliffe 1983 and Keller 1977). Nevertheless, figure 10 provides some useful information in interpreting the cellular-mode exchange process in the context of bifurcation phenomena.

As a stability boundary is crossed, a particular cellular flow mutates into a different one by switching on to another surface. In certain regions of the parameter set several such stable solution surfaces can exist. Therefore, loss of stability of a $2N$-cell mode does not necessarily mean the formation of either a $2(N+1)$-cell or a $2(N-1)$-cell mode.

As illustrated previously, a jump of two or four or six cells is possible. For a situation where only the aspect ratio is adjusted through a stability boundary, the 'end-cell-type' mutation, resulting in a jump of four cells dominates. The 'interior-hot-spot-type' change occurs when Gr is reduced through a stability boundary and can result in a jump of two, four or $2N$ cells depending on the number of hot regions above the bottom wall. Other modes of mutation, which have not been observed in this study, may be possible. In the earlier study by Nandakumar *et al.* (1985), a 'cold-spot-type' bifurcation was found, in which case two cells germinate in the cold downward-flowing region (the vertial bisector) above the bottom wall. This process occurs at a very high Grashof number (about 225000 at $\gamma = 1$) and the resulting cusp points away from the γ-axis. We have not observed a similar process in the present study. At higher values of Gr the flow tends to oscillate. A brief interpretation of the exchange process across the stability boundaries is presented below in the context of bifurcation structures observed for similar problems.

For parametric values (Gr, γ) below curve BA, only the two-cell mode is found to exist. To the right of BA, the four-cell mode is secondary and may be obtained by an impulsive start. To the right of curve CD, the two-cell mode is secondary. If Gr is increased gradually at a γ-value between that of B and C it exhibits two-cell flow to the left of BA until BC is reached, at which point it jumps to a four-cell mode. It remains stable upon further increase of Gr. However, it will collapse to a two-cell mode as the bifurcation curve BA is crossed by gradually reducing Gr. This phenomenon is known as the primary-mode hysteresis which is typical for primary-mode exchange process. Thus the stability boundaries BA and BCD can be interpreted as forming a tilted cusp bounding (Gr, γ)-values where both cellular modes are possible.

The four-cell to six-cell transition occurs between γ-values of 8.5 and 8.7. In the region bounded by FG_1H_1 and a constant γ-line through F, the six-cell mode is secondary and collapses into four-cell flow when Gr is reduced. Four-cell flow may exist as the secondary mode above this region. However, as Gr is reduced through curve GI, it collapses into a six-cell flow. Primary-mode hysteresis occurs when Gr is increased gradually at an aspect ratio betwen 8.5 and 8.7. In this instance, the four-cell mode transforms into six-cell mode when FG is reached. The six-cell mode thus formed collapses back into four-cell flow only when Gr has been reduced below curve FG_1. This primary-mode exchange process again appears to take place through a cusp, though the hysteresis is much less pronounced compared to the two-cell to four-cell transition.

The last cusp region investigated is the six-cell to eight-cell transition. To the right of curve KIL, the eight-cell mode exists as a secondary mode. It mutates to a six-cell flow below curve KI and a four-cell flow below curve IL. Six-cell flow is stable up to curve KL_1MN. Above curve KL_1M, six-cell flow mutates to an eight-cell flow, whereas above curve MN ten-cell flow will form when the aspect ratio is further increased. Primary-mode hysteresis occurs between aspect ratios of 10.9 and 11.8 through the tilted-cusp region IKL_1, which is substantially larger than the four-cell to six-cell cusp.

There is one rather interesting point about the shape of the four-cell upper-limit curve FGIJ. It exhibits a local maximum at I where it is bisected† by the eight-cell lower-limit curve KIL. To the right of curve KIL, the four-cell mode changes into

† Since these bifurcation curves are isolated in the functional space, it is their projections on the (Gr, γ)-plane which are bisecting one another.

the eight-cell mode via the 'end-cell-type' mutation when curve IJ is crossed by increasing the γ-value. However, the eight-cell mode is unstable to the left of curve KIL, and the four-cell mode mutates into the six-cell mode when the γ-value is increased beyond curve FGI. Hence, the four-cell upper stability limit FGIJ may be subdivided into two segments at point I, each representing a particular mutation process. A similar behaviour occurs where the two-cell upper stability limit BCD bisects the six-cell lower stability limit FG_1H at G_1. Along curve G_1H, two-cell flow is formed when the γ-value of an initial six-cell flow is reduced, whereas along curve FG_1 and HH_1, a four-cell flow is generated.

5. Conclusions

Following the lead of Benjamin (1978*a*) in the investigations of boundary effects on the Taylor-vortex instability problem, the mixed-convection heat-transfer problem in rectangular tubes has been studied numerically, recognizing the fact that these problems are similar and will exhibit certain similarities of solution behaviour. We can summarize the findings of this investigation as follows. For rectangular ducts of finite aspect ratios, the appearance of cellular flows via buoyancy instability is gradual and that there is no precise critical value of Gr at which such development occurs abruptly. There is one primary mode that may survive as Gr approaches zero. Other cellular flows can exist at that aspect ratio as secondary modes which collapse to other modes at their stability boundaries. The cellular flows observed in this study are even-cellular modes. None of the odd-cell modes that were observed in Benjamin & Mullin's (1981) Taylor-vortex experiments were established. The primary modes appear to exchange roles via a cusp region. Below the quasi-critical range, only end vortices are present. For the three transitions located (two-to-four-cell, four-to-six-cell, and six-to-eight-cell), they follow qualitatively the sequence of events observed by Benjamin. For the range of parameters studied $Gr \in (1000, 25000)$ and $\gamma \in (4, 16)$, up to four stable solutions can exist for a parametric set (Gr, γ). It is to be expected that multiplicity will increase with increasing γ-value. Two mutation processes, viz. the 'end-cell-type' and the 'interior-hot-spot-type' mutation have been observed.

REFERENCES

ARAKAWA, A. 1966 Computational design for long-term numerical integration of the equations of fluid motion: two-dimensional incompressible flow. Part I. *J. Comp. Phys.* **1**, 119–143.

BEHRINGER, R. P. & AHLERS, G. 1982 Heat transport and temporal evolution of fluid flow near the Rayleigh–Bénard instability in cylindrical containers. *J. Fluid Mech.* **125**, 219–258.

BÉNARD, M. 1901 Les troubillions cellulaires dans une nappe liquide transportant de la chaleur par convection en regime permanent. *Ann. Chim. Phys.* **23**, 62–144.

BENJAMIN, T. B. 1976 Application of Leray–Schauder degree theory to problems of hydrodynamic stability. *Math. Proc. Camb. Phil. Soc.*, **79**, 373–392.

BENJAMIN, T.B. 1978*a* Bifurcation phenomena in steady flow of a viscous liquid. I. Theory. *Proc. R. Soc. Lond.* A **359**, 1–26.

BENJAMIN, T. B. 1978*b* Bifurcation phenomena in steady flow of a viscous liquid. II. Experiments. *Proc. R. Soc. Lond.* A **359**, 27–43.

BENJAMIN, T. B. 1978*c* Application of generic bifurcation theory in fluid mechanics. In *Contemporary Developments in Continuum Mechanics and Partial Differential Equations* (ed. G. M. de la Penha & L. A. J. Madeiros). North-Holland.

BENJAMIN, T. B. & MULLIN, T. 1981 Anomalous modes in the Taylor experiment. *Proc. R. Soc. Lond.* A **337**, 221–249.

BENJAMIN, T. B. & MULLIN, T. 1982 Notes on the multiplicity of flows in the Taylor experiment. *J. Fluid Mech.* **121**, 219–230.

CHENG, K. C. & HWANG, G.-J. 1969 Numerical solution for combined free and forced laminar convection in horizontal rectangular channels. *Trans. ASME.* C: *J. Heat Transfer*, **91**, 59–66.

CHOU, F. C. & HWANG, G.-J. 1984 Combined free and forced laminar convection in horizontal rectangular channels for high *Re-Ra*. *Can. J. Chem. Engng* **62**, 830–836.

CLIFFE, K. A. 1983 Numerical calculation of two-cell and single-cell Taylor flows. *J. Fluid Mech.* **135**, 219–233.

CLIFFE, K. A. & MULLIN, T. 1985 A numerical and experimental study of anomalous modes in the Taylor experiment. *J. Fluid Mech.* **153**, 243–258.

CLIFFE, K. A. & WINTERS, K. H. 1984 A numerical study of the cusp catastrophe for Bénard convection in tilted cavities. *J. Comp. Phys.* **54**, 531–534.

COUTIER, J. P. & GREIF, R. 1985 An investigation of laminar mixed convection inside a horizontal tube with isothermal wall conditions. *Intl J. Heat Mass Transfer* **28**, 1293–1305.

DANIELS, P. G. 1977 The effect of distant sidewalls on the transition to finite amplitude Bénard convection. *Proc. R. Soc. Lond.* A **358**, 173–197.

DANIELS, P. G. 1981 The effect of distant sidewalls on the evolution and stability of finite amplitude Rayleigh–Bénard convection. *Proc. R. Soc. Lond.* A **378**, 539–566.

DANIELS, P. G. 1984 Roll-pattern evolution in finite amplitude Rayleigh–Bénard convection in a two-dimensional fluid layer bounded by distant sidewalls. *J. Fluid Mech.* **143**, 125–152.

DRAZIN, P. G. 1975 On the effects of sidewalls on Bénard convection. *Z. Angew. Math. Phys.* **27**, 239–243.

DUFORT, E. C. & FRANKEL, S. P. 1953 Stability conditions in the numerical treatment of parabolic differential equations. *Math. Tables and Other Aids to Comps.* **7**, 135–152.

FARIS, G. N. & VISKANTA, R. 1969 An analysis of combined forced and free convection heat transfer in a horizontal tube. *Intl J. Heat Mass Transfer* **12**, 1295–1309.

FESTA, J. F. 1970 A numerical model of a convective cell driven by non-uniform horizontal heating. MS thesis, Massachusetts Institute of Technology.

FOIAS, C. & TEMAIN, R. 1977 Structure of the set of stationary solutions of the Navier–Stokes equations. *Commun. Pure Appl. Maths* **30**, 149–164

HALL, P. & WALTON, I. C. 1977 The smooth transition to a convective regime in a two-dimensional box. *Proc. R. Soc. Lond.* A **358**, 199–221.

HATTORI, N. & KOTAKE, S. 1978 Combined free and forced convection heat transfer for fully developed laminar flow in horizontal tubes (experiments). *Bull. JSME* **21**, 861–868.

HORNE, R. N. & O'SULLIVAN, M. J. 1974 Oscillatory convection in a porous medium heated from below. *J. Fluid Mech.* **66**, 339–352.

HWANG, G.-J & CHENG, K. C. 1970 Boundary vorticity method for convective heat transfer with secondary flow-application to the combined free and forced laminar convection in horizontal tubes. *Heat Transfer*, vol. 4, Paper No. NC3-5.

HWANG, G.-J & LIU, C.-L. 1976 An experimental study of convective instability in the thermal entrance region of a horizontal parallel plate channel heated from below. *Can. J. Chem. Engng* **54**, 521–525.

IQBAL, M. & STACHIEWICZ, J. W. 1966 Influence of tube orientation on combined free and forced laminar convection heat transfer. *Trans. ASME* C: *J. Heat Transfer* **88**, 109–116.

IQBAL, M. & STACHIEWICZ, J. W. 1967 Variable density effects in combined free and forced convection in inclined tubes. *Intl J. Heat Mass Transfer* **10**, 1625–1629.

JEFFREYS, H. 1928 Some cases of instability in fluid motion. *Proc. R. Soc. Lond.* A **118**, 195–208.

KELLER, H. B. 1977 Numerical solutions of bifurcation and nonlinear eigenvalue problems. In *Applications of Bifurcation Theory* (ed. P. H. Rabinowitz), pp. 359–384. Academic.

LEE, Y. & KORPELA, S. A. 1983 Multicellular natural convection in a vertical slot. *J. Fluid Mech.* **126**, 91–121.

LINTHORST, S. J. M., SCHINKEL, W. M. M. & HOOGENDOORN, C. J. 1980 Natural convection flow in inclined air-filled enclosures of small and moderate aspect ratio. *Proc. 2nd Intl Symp. on Flow Visualization, Bochum, West Germany* (ed. W. Merzkirch), pp. 93–97.

LOW, A. R. 1929 On the criterion for stability of a layer of viscous fluid heated from below. *Proc. R. Soc. Lond.* A **125**, 180–195.

MASLIYAH, J. H. 1980 On laminar flow in curved semi-circular ducts. *J. Fluid Mech.* **99**, 469–479.

MEYER-SPASCHE, R. & KELLER, H. B. 1985 Some bifurcation diagrams for Taylor vortex flows. *Phys. Fluids* **28**, 1248–1252.

MORTON, B. R. 1959 Laminar convection in uniformly heated horizontal pipes at low Rayleigh numbers. *Q. J. Mech. Appl. Maths.* **12**, 410–420.

MULLIN, T. 1982 Mutations of steady cellular flows in the Taylor experiment. *J. Fluid Mech.* **121**, 207–218.

NANDAKUMAR, K., MASLIYAH, J. H. & LAW, H.-S. 1985 Bifurcation in steady laminar mixed convection flow in horizontal rectangular tubes. *J. Fluid Mecch.* **152**, 145–161.

OSBORNE, D. G. & INCROPERA, F. P. 1985 Laminar mixed convection heat transfer for flow between horizontal parallel plates with asymmetric heating. *Intl J. Heat Mass Transfer* **28**, 207–217.

PATANKAR, S. B., RAMADHYANI, S. & SPARROW, E. M. 1978 Effect of circumferentially non-uniform heating on laminar combined convention in a horizontal tube. *Trans. ASME* C: *J. Heat Transfer* **100**, 63–70.

PLATTEN, J. K. & CHAVEPEYER, G. 1975 An hysteresis loop in the two component Bénard problem. *Intl. J. Heat Mass Transfer* **18**, 1071–1075.

QUON, C. 1977 Free convection in enclosure revisited. *Trans. ASME* C: *J. Heat Transfer* **99**, 340–342.

RAYLEIGH, LORD 1916 On convection currents in a horizontal layer of fluid when the higher temperature is on the underside. *Scientific Papers*, vol. 6, pp. 432–446. Cambridge University Press.

ROACHE, P. J. 1972 *Computational Fluid Dynamics.* Hermosa.

SCHAEFFER, D. G. 1980 Qualitative analysis of a model for boundary effects in the Taylor problem. *Math. Proc. Camb. Phil. Soc.* **87**, 307–377.

WINTERS, K. H. & BRINDLEY, R. C. G. 1984 Multiple solutions for laminar flow in helically-coiled tubes. *Harwell Rep.* AERE-R 11373.

WIRTZ, R. A. & LIU, L. H. 1975 Numerical experiments on the onset of layered convection in a narrow slot containing a stably stratified fluid. *Intl J. Heat Mass Transfer* **18**, 1299–1305.

YOUSEF, W. W. & TARASUK, J. D. 1981 An interferometric study of combined free and forced convection in a horizontal isothermal tube. *Trans. ASME* C: *J. Heat Transfer* **103**, 249–256.